

# Aligned Rectangular Few-Layer Graphene Domains on Copper Surfaces

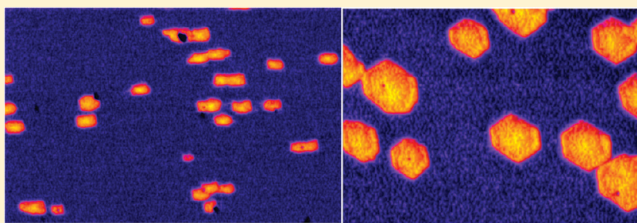
Yimin A. Wu, Alex W. Robertson, Franziska Schäffel, Susannah C. Speller, and Jamie H. Warner\*

Department of Materials, University of Oxford, Parks Road, Oxford OX1 3PH, United Kingdom

**S** Supporting Information

**ABSTRACT:** We show that aligned rectangular few layer graphene (FLG) domains can be produced on Cu surfaces using atmospheric pressure chemical vapor deposition. For the growth temperatures of 990 and 1000 °C the FLG domains are primarily hexagonal in shape, but at 980 °C, morphology transition of FLG domains is observed associated with different Cu grains. Rectangular FLG domains are synthesized for the first time and we show using electron backscattered diffraction that they only grow on Cu grains with (111) orientation because of the interplay between the atomic structure of the Cu lattice and the graphene domains. We show that hexagonal FLG domains can form on nearly all other non-(111) Cu surfaces. These results indicate that even at atmospheric pressure, the interplay between the Cu atomic structure and graphene formation can be strong and lead to aligned rectangular domains.

**KEYWORDS:** graphene, APCVD, copper, morphology, alignment



## INTRODUCTION

Metal-assisted chemical vapor deposition (CVD) has attracted intensive attention for its capability of producing large area graphene films that have potential for integration with current CMOS technology,<sup>1–4</sup> and as transparent conducting electrodes.<sup>5–7</sup> Low-pressure (LP) CVD synthesis of graphene on Cu has demonstrated excellent results in producing monolayer<sup>8–10</sup> and bilayer graphene.<sup>11,12</sup> The mechanism of graphene growth by LP-CVD has been studied by isotope labeling<sup>13</sup> and a two-step CVD process.<sup>14</sup> Recently, the progress of the synthesis of graphene using atmospheric pressure (AP) CVD<sup>15–18</sup> has shown the growth is not always self-limiting to monolayer graphene and indicates complex growth dynamics are at play.

Growth of graphene at atmospheric pressure has the benefit of not needing vacuum conditions that are harder to implement on the large scale necessary for industrial development. To date, there is very little knowledge regarding how the Cu lattice plays a role for the growth dynamics of graphene and few-layer graphene (FLG) on Cu foils using AP-CVD. Wofford et al. investigated the interplay of Cu foil and graphene under low pressure (LP) by in situ low-energy electron microscopy.<sup>9</sup> They found that four-lobe polycrystalline graphene domains grew on a pronounced Cu (100) textured surface with random orientation to the Cu grain.<sup>9</sup> A growth mode dominated by edge kinetics with an angular dependent growth velocity is suggested as the growth mechanism for this type of four lobe polycrystalline graphene,<sup>9</sup> which is also observed by the work of the Ruoff group.<sup>13,14</sup> Rasool et al. studied the continuity of graphene on polycrystalline copper synthesized by LP-CVD.<sup>19</sup> They suggest the morphology and atomic arrangement of the underlying Cu foil do not affect the atomic arrangement of graphene.<sup>19</sup> The growth of graphene on single crystal Cu (111) in an ultrahigh vacuum chamber has been

studied by scanning tunnelling microscopy.<sup>20</sup> They find the random shapes of graphene domains nucleate on Cu lattice with either 7 or 0° misorientation angle, which leads to numerous domain boundaries when domains emerge into continuous film.<sup>20</sup> This can dramatically reduce the carrier mobility of graphene grown by LP-CVD.<sup>20</sup> Zhao et al. studied the graphene grown on Cu (111) and (100) under high vacuum by STM.<sup>21</sup> They found that graphene had a hexagonal superstructure on Cu (111), whereas a linear superstructure appeared on Cu (100).<sup>21</sup>

Here, we investigate the role Cu lattice has on the growth dynamics of FLG domains at atmospheric pressures in CVD. We show that reducing the growth temperature from 1000 °C down to 980 °C changes the growth dynamics of the system and enables the Cu lattice to start to play a role in the crystal growth. We show for the first time the growth of aligned rectangular shaped FLG domains that form only on Cu (111) grains at 980 °C. Hexagonal FLG domains are shown to grow on nearly all non-(111) Cu lattice planes. This reveals that the atomic structure of Cu does indeed play a role in the growth dynamics of graphene even at atmospheric pressure when the conditions such as temperature are appropriate.

## EXPERIMENTAL SECTION

**Atmospheric Pressure (AP) CVD Growth of Few-Layer Graphene.** One square centimeter copper foils of 99.999% purity and 0.1 mm thickness (Alfa Aesar) were loaded into a quartz tube and rested just outside the hot zone in a horizontal split-tube furnace. After the whole system was purged with argon gas, volume ratio 1:3 H<sub>2</sub>:Ar gas

**Received:** June 27, 2011

**Revised:** July 30, 2011

**Published:** September 20, 2011

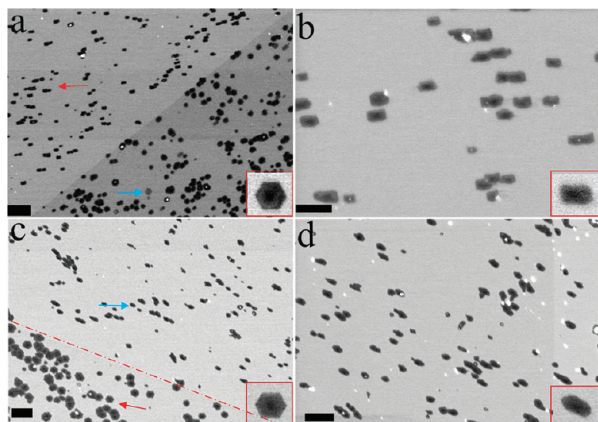


**Figure 1.** SEM images of Cu grain effect on shape control of the nucleation of graphene domains: (a) Rectangular-shaped (red arrow) and hexagonal-shaped (blue arrow) FLG domains nucleated on different Cu grains at 980 °C. Inset in bottom right shows a single hexagon. (b) Higher-magnification image of the rectangular-shaped FLG domains at 980 °C. (c) Hexagonal-shaped (red arrow) and nonfaceted elongated (blue arrow) FLG domains nucleated on different Cu grains at 990 °C. Inset in bottom right shows a single hexagon. (d) Higher-magnification image of elongated nonfaceted FLG domains at 990 °C. The scale bars in a–d are 2, 1, 2, and 2  $\mu\text{m}$ , respectively. Insets show individual domains.

mix at 600 sccm flow was introduced into the system and continued throughout the graphene synthesis and cooling. The temperature of the furnace was adjusted to the desired value for annealing and growth (i.e., 1000, 990, and 980 °C). Once the furnace reached the desired temperature, the quartz tube was shifted so that the copper foil was moved to the hot-zone in the furnace, where it was annealed and reduced for 0.5 h hydrogen pretreatment time. Then, volume ratio 1:4  $\text{CH}_4$ :Ar gas mix was introduced at a flow rate of 10 sccm for 3 min growth time. It means the volume ration is 1:75:229  $\text{CH}_4$ : $\text{H}_2$ :Ar during the reaction. The sample was then rapidly cooled to room temperature with an average cooling rate of 40 °C/min (see the Supporting Information) by removing them from the hot zone of the furnace under a hydrogen and argon atmosphere.

**Characterization.** Scanning electron microscopy (SEM) was performed with a Zeiss NVision 40 FIB-SEM operating at 2 kV. Electron backscatter diffraction (EBSD) measurements were performed with JEOL 6500F at 20 kV. Raman spectra were taken using a JY Horiba Labram Aramis imaging confocal Raman microscope with a 532 nm frequency doubled Nd:YAG laser. Transmission electron microscopy and selective area electron diffraction were performed using a JEOL 4000EX TEM operating at an accelerating voltage of 80 kV.

## RESULTS AND DISCUSSION

Well-defined hexagonal single-crystal FLG domains have been previously grown by AP-CVD using Cu foils of 99.8% purity at a growth temperature of 1000 °C.<sup>22,23</sup> Cu foils of 99.8% purity were also used in many other reports of CVD growth by the Ruoff group.<sup>7,8,10,13,14</sup> However, we found that when using these 99.8% Cu films, the graphene nucleation is dominated by impurities on the surface and mechanical deformations (see the Supporting Information). In this report we focus on using higher quality Cu foils of 99.999% purity and increased thickness from 0.025 to 0.1 mm as they enable the true interplay between the graphene domains and the Cu atomic structure to be revealed because the artificial nucleation points that are prevalent on 99.8% Cu foils are greatly reduced. The temperature of the furnace was

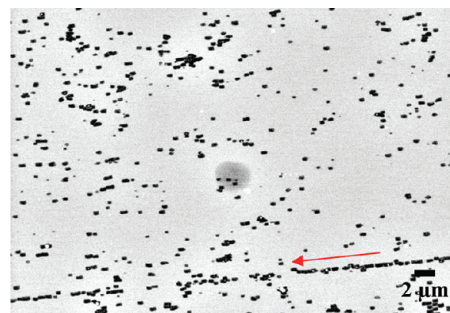


**Figure 2.** SEM image showing alignment of rectangular-shaped few-layer graphene domains over a region of 44  $\mu\text{m} \times 30 \mu\text{m}$ , indicated by red arrow.

adjusted to the desired value for annealing and carbon source deposition. The Cu foils were annealed in 1:3  $\text{H}_2$ :Ar gas mix at 600 sccm flow for 0.5 h hydrogen pretreatment time. During a growth time of 3 min 1:4  $\text{CH}_4$ :Ar gas mixture was applied at a flow rate of 10 sccm. The samples were rapidly cooled to room temperature by removing from the hot zone of the furnace after the growth time.

Figure 1a shows the grain boundary between two Cu grains for a growth temperature of 980 °C. Figure 1a shows rectangular shaped FLG domains on the brighter contrast left sided Cu grain (red arrow), whereas hexagonal shaped FLG domains form on the darker contrast right sided region (blue arrow) with an inset showing an individual hexagonal domain. The nucleation density in these two Cu grains is similar but the size of the domains is different. The nucleation density in the light contrast grain is  $\sim 0.42 \mu\text{m}^{-2}$ , whereas the nucleation density in the dark contrast grain is  $\sim 0.47 \mu\text{m}^{-2}$ . The higher-magnification SEM image of rectangular shaped FLG domains is presented in Figure 1b with an inset showing an individual rectangular domain. Some shape variations of FLG domains were also observed at 990 °C, shown in Figure 1c. However, this was only a minor deviation from the predominant hexagonal shapes. Hexagonal FLG domains are seen in the lower left region on one Cu grain (red arrow) with an inset showing single domain in Figure 1c, whereas elongated FLG domains that lack faceting are observed on the other larger Cu grain (blue arrow). The higher-magnification image of the elongated nonfaceted FLG domains is shown in Figure 1d with an inset showing a single domain. In images a and c in Figure 1, the Cu grain boundary does not contain a larger proportion of FLG domains, indicating that it does not always act as a nucleation site for growth.<sup>9</sup> The Raman spectra corresponding to images a and c in Figure 1 is shown in the Supporting Information. Transmission electron microscopy and selected area electron diffraction analysis of FLG domains transferred onto TEM grids indicated the domains were single crystals (see the Supporting Information). At growth temperatures of 1000 °C, all FLG domains were hexagonal, indicating that the Cu lattice no longer affected the shape of domains. Lowering the temperature further to 970 °C led to reduced quality of FLG domains because of a decrease in the catalytic activity of the system. This indicates that a critical temperature of 980 °C is required to get optimized Cu-FLG interactions. The rectangular-shaped FLG domains were also aligned in their orientation. Figure 2 shows a SEM image of a large 44  $\mu\text{m} \times 30 \mu\text{m}$  area of aligned rectangular FLG domains with the red arrow indicating the direction of orientation of the domains.



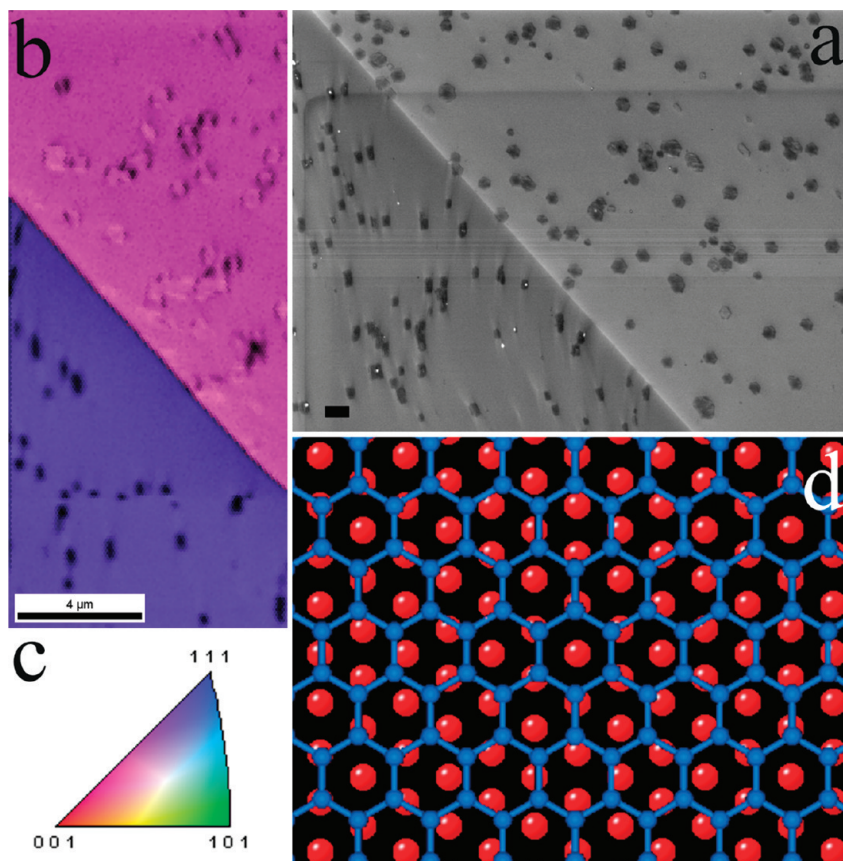


**Figure 3.** (a) SEM image shows two Cu grains associated with hexagonal or rectangular graphene domains, respectively. (b) EBSD mapping of the region shown in panel a. The scale bar is 1 μm. (c) Color key used to index the EBSD mapping in Figures 3 and 4. (d) Atomic model of graphene on Cu (111), corresponding to the blue region in panel b. The blue atoms are carbon and red atoms are Cu.

To understand why the FLG domains changed shape from hexagonal to rectangular across different Cu grains, electron backscatter diffraction (EBSD) was used to measure the orientation of the Cu crystal structure in the regions of FLG shape change. When measuring the EBSD, the sample was tilted 70° from the horizontal plane, the graphene samples will have different contrast on different Cu crystal plane. Figure 3a shows the SEM image of the boundary region between two Cu grains, on which hexagonal (right) and rectangular (left) shaped FLG domains are grown. SEM contrast features were observed to surround the rectangular FLG domains but not the hexagonal FLG domains, and were attributed to deformation caused by the stress in the Cu crystal induced by the FLG domains. EBSD analysis has been carried out on a region surrounding the boundary in Figure 3a. The map in Figure 3b shows the orientation of the Cu crystal lattice relative to the sample normal direction superimposed on the secondary electron image, color according to the key in Figure 3c. The blue Cu grain in Figure 3b is a Cu (111) plane, on which the rectangular FLG domains are produced. The pink Cu grain in Figure 3b is associated with hexagonal FLG graphene domains and is a higher index plane between Cu (111) and (001). We found that the rectangular-shaped FLG domains were only produced on the Cu (111) surfaces, whereas hexagonal-shaped FLG domains were produced on all other Cu surfaces, which is shown in Figure 4.

Figure 3d shows an atomic model of graphene on the Cu (111) plane, which is corresponding to the blue region in

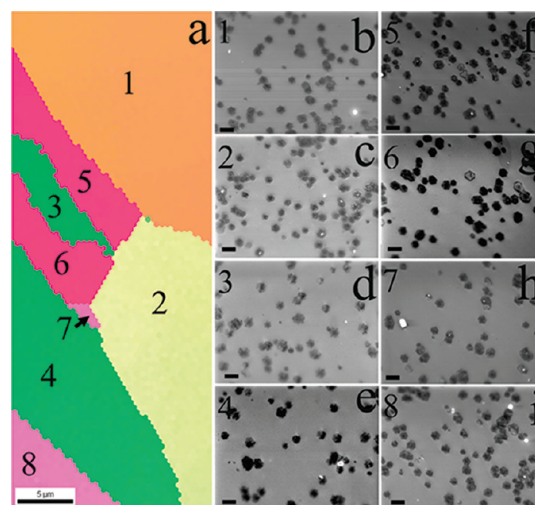


**Figure 4.** (a) EBSD mapping of another area containing eight Cu grains, which are labeled with numbers 1–8. (b–i) SEM images labeled with 1–8 correspond to the FLG grown on the Cu grains labeled with 1–8 in panel a, respectively. The scale bars of all SEM images are 1 μm.

Figure 3a. A previous STM study shows the lattice of graphene is either strictly aligned with Cu (111) or with 7° misorientation angle with respect to the Cu lattice synthesized by LP-CVD.<sup>20</sup> However, in that report, random shapes of graphene domains

were produced on Cu (111) by LP-CVD.<sup>20</sup> The Cu (111) surface has 6 fold symmetry and a graphene lattice has 6-fold symmetry, but the resulting rectangular shaped FLG domains produced are 2 fold symmetric. The interatomic spacing of Cu atoms on a (111) surface is typically 0.148 nm, whereas the C–C separation in sp<sup>2</sup>-bonded graphene is typically 0.142 nm leads to a small ~4% lattice mismatch between the graphene and copper surface and may lead to some strain in the system.<sup>23</sup> The elongated direction of the rectangle FLG domain has faster growth kinetics than the shorter direction and thus 2-fold symmetry is produced.

Figure 4a shows a normal direction EBSD map of another area that contained eight different Cu grains with labels 1–8. The orientation of the sample normal direction in each grain can be identified using the color key in Figure 3c. The results in Figure 4a suggest that green Cu grains with labels 3–4 are Cu (101) plane, whereas the red grains with labels 5–6 are Cu (001) plane. The orange (label 1) and yellow (label 2) grains are high index planes between Cu (001) and (101). The pink grains labeled with 7–8 are higher index planes between Cu (001) and (111). SEM images corresponding to each individual Cu grain in Figure 4a are shown in Figure 4b–i with the same label number as the grains. It is interesting to note that only hexagonal FLG domains were grown on all these Cu grains, although they are different Cu lattice planes.

Alignment due to the direction of gas flow can be ruled out as a cause. This is because within the one sheet of Cu, the direction of graphene domain alignment varies from Cu grain to grain, because of the variation in the relative orientation of the different Cu grains. Within one Cu grain, graphene domains are aligned. This indicates that the mechanism for alignment is the relationship between the atomic structure of the Cu and the growing graphene, along with the role hydrogen plays in forming faceted structures. Because Cu (111) and the graphene hexagonal lattice are both 6 fold symmetric, it is surprising that this leads to a 2-fold symmetric rectangular graphene structure. The observation of strain in the Cu surrounding the rectangular domains suggests the situation is more complicated as the atomic structure of the underlying Cu (111) surface is distorted by the presence of graphene and this may lead to a growth direction that has lower energy and faster kinetics, or conversely a direction where hydrogen is more effective at etching away carbon atoms from the edge of the graphene domain, slowing growth in this direction. It is hard to predict the exact effect that atomic defects in the Cu lattice will have on the shape change and alignment, apart from being sites where nucleation of graphene domains may occur.

The different kinetics of this catalytic reaction on Cu (111) is the direct reason for the formation and alignment of the rectangular graphene domains. The different kinetics can be affected by the crystal structure of Cu (111), dislocations, or other reasons like hydrogen partial pressure. Vlasiouk et al. studied the role of hydrogen partial pressure in controlling the size and morphology of graphene domains.<sup>24</sup> It is possible that hydrogen partial pressure plays a role in affecting the catalytic efficiency, and optimum temperature for the formation of various shapes of graphene domains.

From our study, it is clear that by reducing nucleation from impurities and improving the surface quality of the Cu foils it is possible to observe strong interactions between the atomic structure of Cu and the growth dynamics of graphene even at atmospheric pressures. The different growth kinetics on a

Cu (111) plane in AP-CVD lead to aligned rectangular shaped single crystal FLG domains, rather than hexagonal domains. These results suggest that the Cu lattice is an important factor in the mechanism of graphene formation in AP-CVD and can be used to align polycrystalline domains in a 2D film and potentially reduce the effect of domain boundaries. By engineering Cu foil with a dominant (111) plane it could lead to large area formation of rectangular shape of graphene domains, which might exhibit interesting physics.

## CONCLUSION

In summary, we have shown for the first time that a morphology transition of micrometer sized FLG domains from hexagonal to rectangular shape on 99.999% purity Cu foil at atmospheric pressure CVD (AP-CVD) using methane at 980 °C. The growth of hexagonal FLG domains is driven by the 6-fold symmetry of the graphene lattice, while the growth of rectangular FLG domains is heavily influenced by the Cu (111) plane. With the possibility of engineering Cu lattice planes on the foil to control the interplay between graphene and Cu, it may be possible to fabricate large area graphene films with improved carrier mobility because of its shape control and large-scale alignment. This may pave the way for better-quality graphene-based electronics.

## ASSOCIATED CONTENT

**S Supporting Information.** The Raman spectra of 980, 990, and 1000 °C samples (Figure S1); SEM images showing the effect of changing from 99.8 to 99.999% purity Cu films (Figure S2); selective area electron diffraction of 980, 990, and 1000 °C sample and HRTEM images of the thickness of graphene domains (Figure S3); plot of the time dependence of experimental growth parameters (Figure S4). This material is available free of charge via the Internet at <http://pubs.acs.org>.

## AUTHOR INFORMATION

### Corresponding Author

\*E-mail: [Jamie.warner@materials.ox.ac.uk](mailto:Jamie.warner@materials.ox.ac.uk).

## ACKNOWLEDGMENT

Y.A.W. acknowledges financial support from EPSRC International Doctoral Scholarship (IDS), Wolfson China Scholarship, China Oxford Scholarship Fund, and Overseas Research Scholarship. F.S. thanks the Alexander von Humboldt Foundation, the BMBF, and EPSRC (EP/F048009/1). J.H.W. thanks the Royal Society for support.

## REFERENCES

- (1) Novoselov, K. S.; Geim, A. K.; Morozov, S. V.; Jiang, D.; Zhang, Y.; Dubonos, S. V.; Grigorieva, I. V.; Firsov, A. A. *Science* **2004**, *306*, 666–669.
- (2) Lemme, M. C.; Echtermeyer, T. J.; Baus, M.; Kurz, H. *IEEE Electron Device Lett.* **2007**, *28*, 282–284.
- (3) Meric, I.; Bklitskaya, N.; Kim, P.; Shepard, K. L. *IEDM Technical Digest*; proceedings from the 2008 Electron Devices Meeting, San Francisco, CA, Dec 15–17, 2008; IEEE: Piscataway, NJ, 2008, paper 21.2.
- (4) Schwierz, F. *Nat. Nanotechnol.* **2010**, *5*, 487–496.
- (5) Kim, K. S.; Zhao, Y.; Jang, H.; Lee, S. Y.; Kim, J. M.; Kim, K. S.; Ahn, J. H.; Kim, P.; Choi, J. Y.; Hong, B. H. *Nature* **2009**, *457*, 706–710.

- (6) Bae, S.; Kim, H.; Lee, Y.; Xu, X.; Park, J. S.; Zheng, Y.; Balakrishnan, J.; Lei, T.; Kim, H. R.; Song, Y. I.; Kim, Y. J.; Kim, K. S.; Özyilmaz, B.; Ahn, J. H.; Hong, B. H.; Iijima, S. *Nat. Nanotechnol.* **2010**, *5*, 574–578.
- (7) Li, X.; Zhu, Y.; Cai, W.; Borysiak, M.; Han, B.; Chen, D.; Piner, R. D.; Colombo, L.; Ruoff, R. S. *Nano Lett.* **2009**, *9* (12), 4359–4363.
- (8) Li, X.; Cai, W.; An, J.; Kim, S.; Nah, J.; Yang, D.; Piner, R.; Velamakanni, A.; Jung, L.; Tutuc, E.; Banerjee, S. K.; Colombo, L.; Ruoff, R. S. *Science* **2009**, *324*, 1312–1314.
- (9) Wofford, J. M.; Nie, S.; McCarty, K. F.; Bartelt, N. C.; Dubon, O. D. *Nano Lett.* **2010**, *10*, 4890–4896.
- (10) Li, X.; Magnuson, C. W.; Venugopal, A.; Tromp, R. M.; Hannon, J. B.; Vogel, E. M.; Colombo, L.; Ruoff, R. S. *J. Am. Chem. Soc.* **2011**, *133*, 2816–2819.
- (11) Lee, S.; Lee, K.; Zhong, Z. *Nano Lett.* **2010**, *10*, 4702–4707.
- (12) Yan, K.; Peng, H.; Zhou, Y.; Li, H.; Liu, Z. *Nano Lett.* **2011**, *11*, 1106–1110.
- (13) Li, X.; Cai, W.; Colombo, L.; Ruoff, R. S. *Nano Lett.* **2009**, *9*, 4268–4272.
- (14) Li, X.; Magnuson, C. W.; Venugopal, A.; An, J.; Suk, J. W.; Han, B.; Borysiak, M.; Cai, W.; Velamakanni, A.; Zhu, Y.; Fu, L.; Vogel, E. M.; Voelkl, E.; Colombo, L.; Ruoff, R. S. *Nano Lett.* **2010**, *10*, 4328–4334.
- (15) Reina, A.; Jia, X.; Ho, J.; Nezich, D.; Son, H.; Bulovic, V.; Dresselhaus, M. S.; Kong, J. *Nano Lett.* **2009**, *9*, 30–35.
- (16) Bhaviripudi, S.; Jia, X.; Dresselhaus, M. S.; Kong, J. *Nano Lett.* **2010**, *10*, 4128–4133.
- (17) Yao, Y.; Li, Z.; Lin, Z.; Moon, K.-S.; Agar, J.; Wong, C. P. *J. Phys. Chem. C* **2011**, *115*, 5232–5238.
- (18) Luo, Z.; Lu, Y.; Singer, D. W.; Berck, M. E.; Somers, L. A.; Goldsmith, B. R.; Johnson, A. T. C. *Chem. Mater.* **2011**, *23*, 1441–1447.
- (19) Rasool, H. I.; Song, E. B.; Allen, M. J.; Wassei, J. K.; Kaner, R. B.; Wang, K. L.; Weiller, B. H.; Gimzewski, J. K. *Nano Lett.* **2011**, *11*, 251–256.
- (20) Gao, L.; Guest, J. R.; Guisinger, N. P. *Nano Lett.* **2010**, *10*, 3512–3516.
- (21) Zhao, L.; Rim, K. T.; Zhou, H.; He, R.; Heinz, T. F.; Pinczuk, A.; Flynn, G. W.; Pasupathy, A. N. *Solid State Commun.* **2011**, *151*, 509–513.
- (22) Robertson, A. W.; Warner, J. H. *Nano Lett.* **2011**, *11*, 1182–1189.
- (23) Bi, H.; Huang, F.; Liang, J.; Xie, X.; Jiang, M. *Adv. Mater.* **2011**, *23*, 3202–3206.
- (24) Vlasiouk, I.; Regmi, M.; Fulvio, P.; Dai, S.; Datskos, P.; Eres, G.; Smirnov, S. *ACS Nano* **2011**, *5*, 6069–6076.